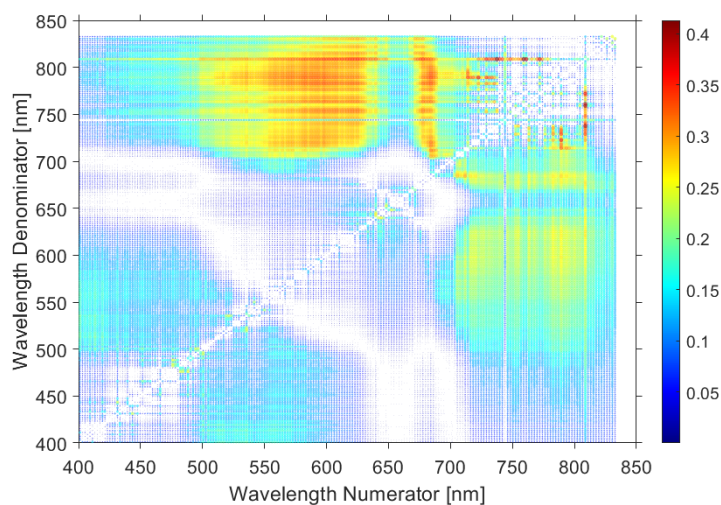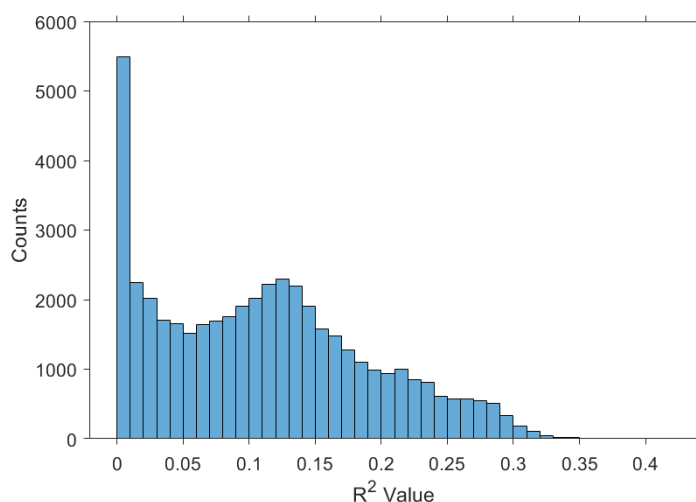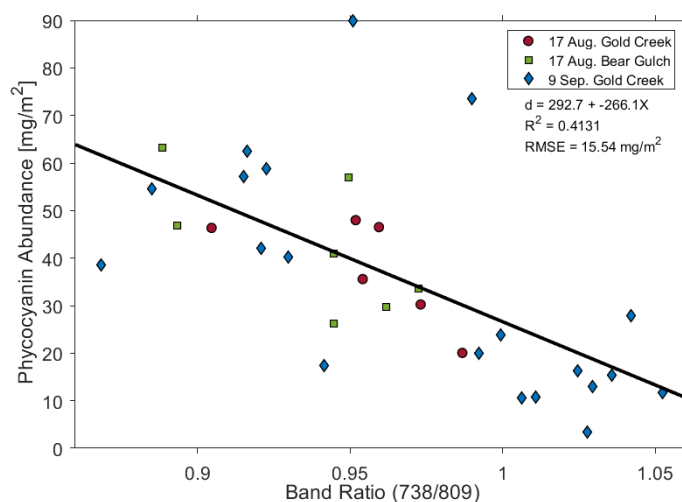# Supplementary Materials:

(a) Heat map of R^2 values generated by fitting each band combination against total phycocyanin standing crops. Colors within the heat map represent the R^2 value, with wavelength numerators and denominators shown on the x- and y-axes, respectively.
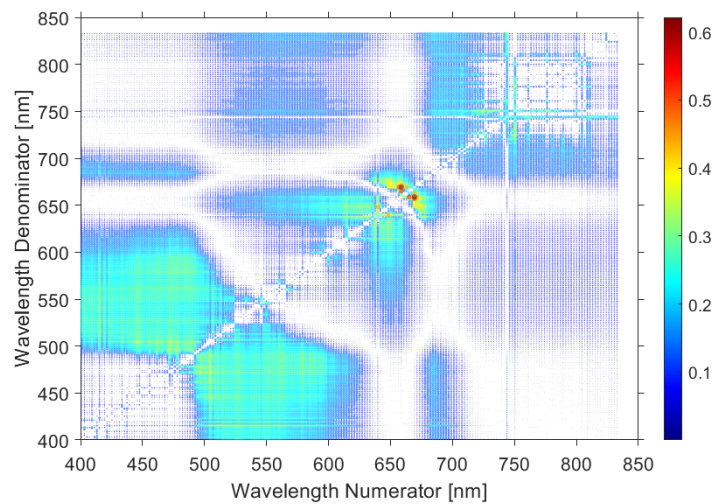

(b) Histogram of the R^2 values generated using the brute-force analysis.
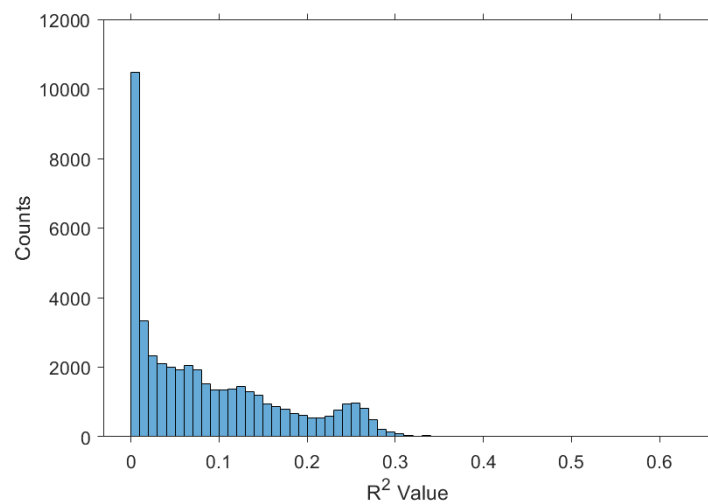

(c) Linear regression analysis between total phycocyanin abundance (y-axis) and optimal band ratio (x-axis). Data collected on 17 August 2021 at the Gold Creek and Bear Gulch site represented by red circles and green squares, respectively, while data collected on 9 September 2021 are shown with blue diamonds.
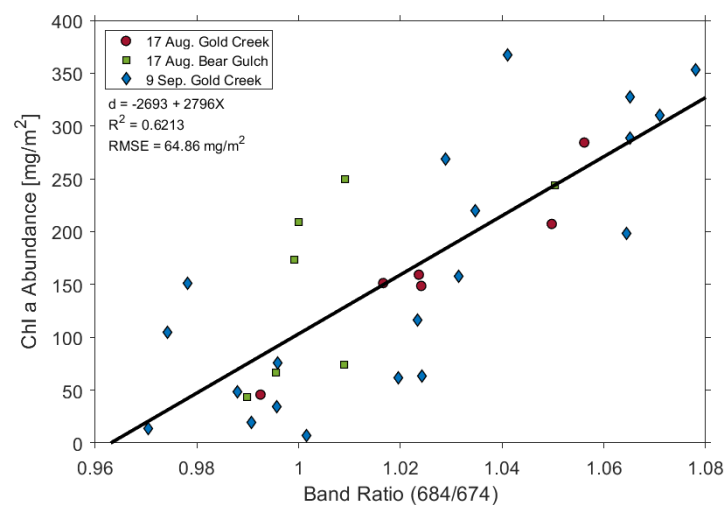
Figure S1. Analytics from the regression analysis of total phycocyanin standing crops from the combined (all field sites) data set.

(a) Heat map of R^2 values generated by fitting each band combination against fila/epip chl *a* standing crops. Colors within the heat map represent the R^2 value, with wavelength numerators and denominators shown on the x- and y-axes, respectively.
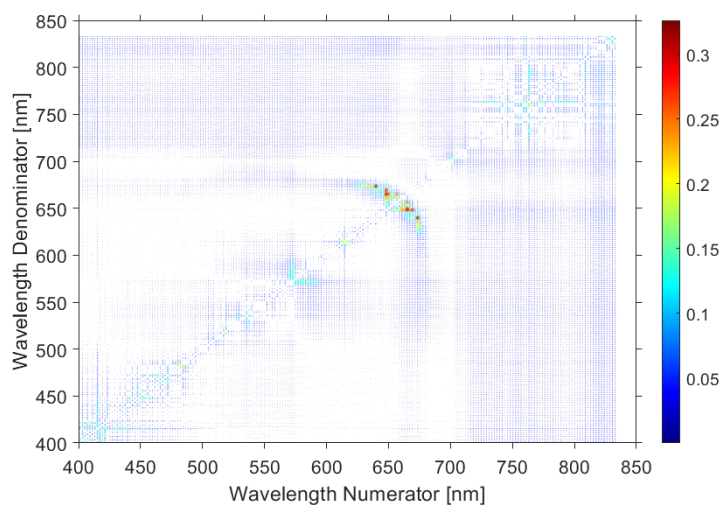

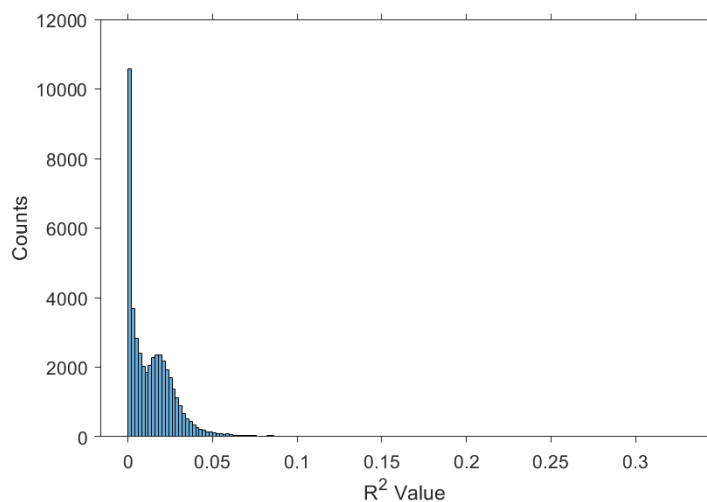(b) Histogram of the R^2 values generated using the brute-force analysis.

(c) Linear regression analysis between chl *a* abundance (y-axis) and optimal band ratio (x-axis). Data collected on 17 August 2021 at the Gold Creek and Bear Gulch site represented by red circles and green squares, respectively, while data collected on 9 September 2021 are shown with blue diamonds.
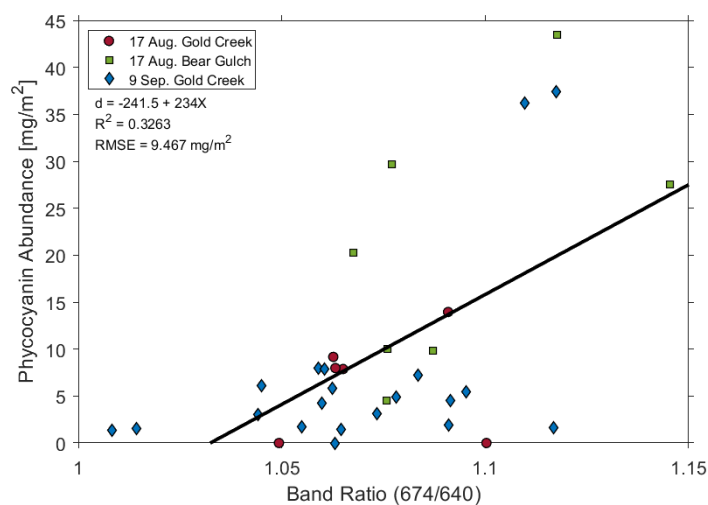
Figure S2. Analytics from the regression analysis of fila/epip chl *a* standing crops from the combined (all field sites) data set.

(a) Heat map of R^2 values generated by fitting each band combination against epiphytic phycocyanin standing crops. Colors within the heat map represent the R^2 value, with wavelength numerators and denominators shown on the x- and y-axes, respectively.
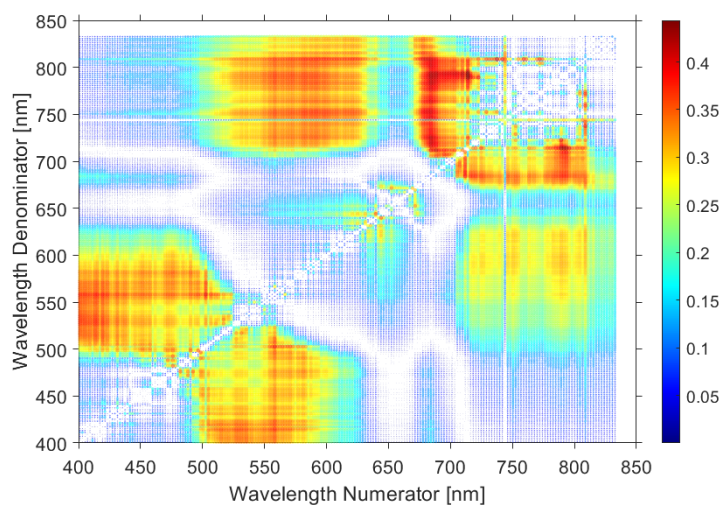

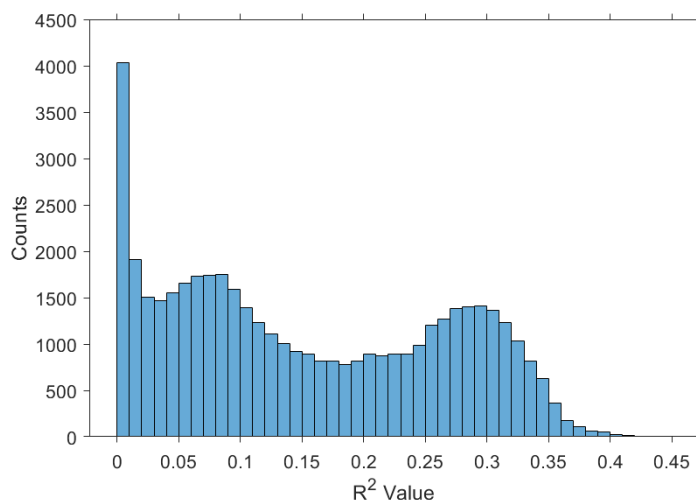(b) Histogram of the R^2 values generated using the brute-force analysis.

(c) Linear regression analysis between phycocyanin abundance (y-axis) and optimal band ratio (x-axis). Data collected on 17 August 2021 at the Gold Creek and Bear Gulch site represented by red circles and green squares, respectively, while data collected on 9 September 2021 are shown with blue diamonds.
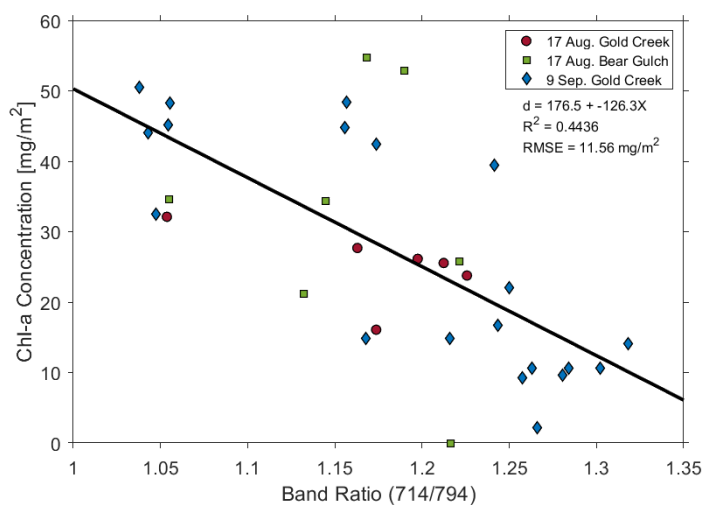
Figure S3. Analytics from the regression analysis of epiphytic phycocyanin standing crops from the combined (all field sites) data set.

(a) Heat map of R^2 values generated by fitting each band combination against epilithic chl *a* standing crops. Colors within the heat map represent the R^2 value, with wavelength numerators and denominators shown on the x- and y-axes, respectively.
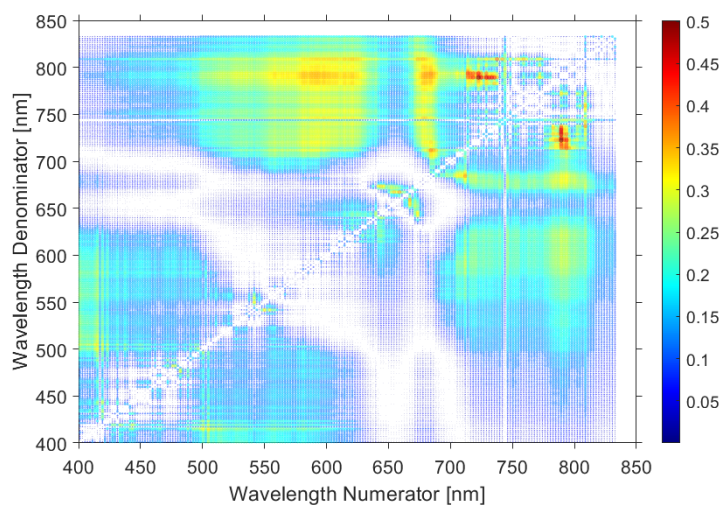

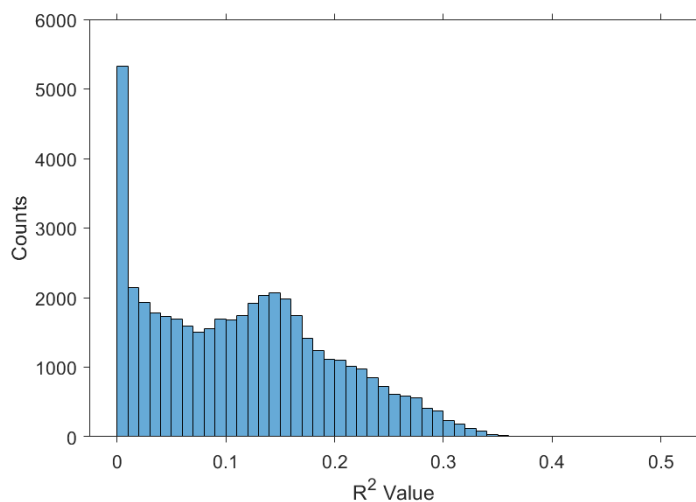(b) Histogram of the R^2 values generated using the brute-force analysis.

(c) Linear regression analysis between epilithic chl *a* abundance (y-axis) and optimal band ratio (x-axis). Data collected on 17 August 2021 at the Gold Creek and Bear Gulch site represented by red circles and green squares, respectively, while data collected on 9 September 2021 are shown with blue diamonds.
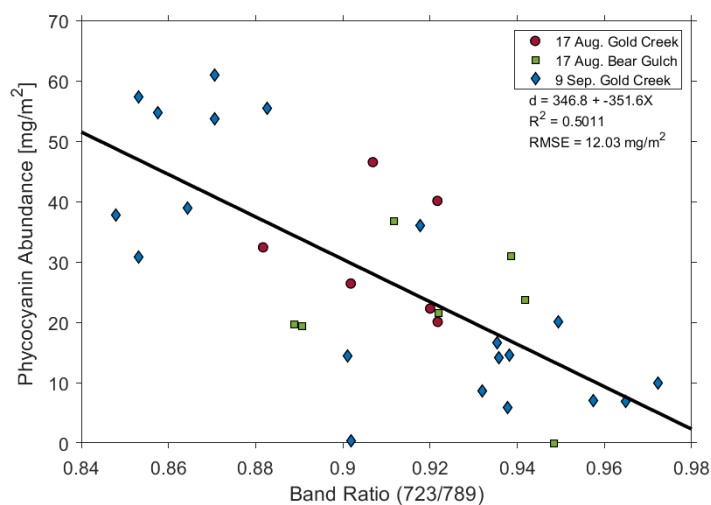
Figure S4. Analytics from the regression analysis of epilithic chl *a* standing crops from the combined (all field sites) data set.

(a) Heat map of R^2 values generated by fitting each band combination against epilithic phycocyanin standing crops. Colors within the heat map represent the R^2 value, with wavelength numerators and denominators shown on the x- and y-axes, respectively.
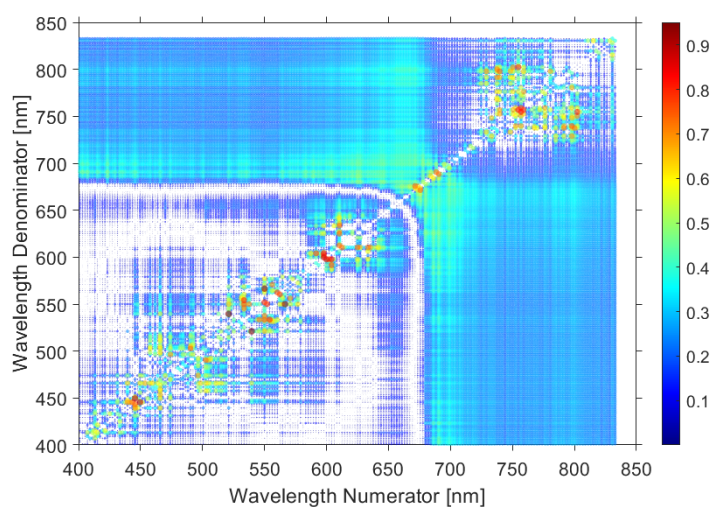

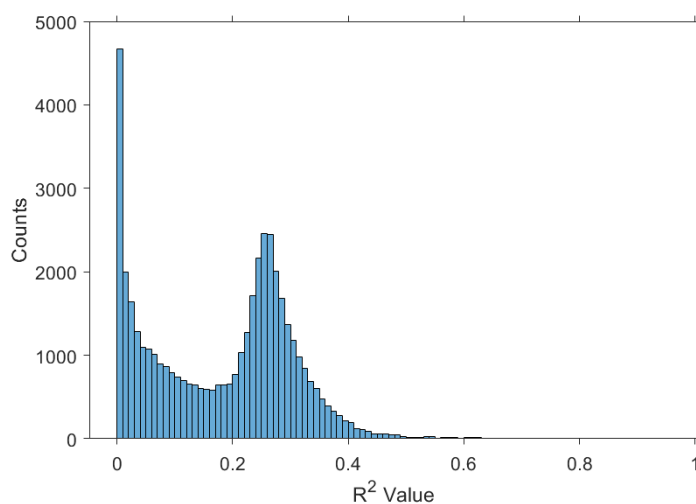(b) Histogram of the R^2 values generated using the brute-force analysis.

(c) Linear regression analysis between epilithic phycocyanin abundance (y-axis) and optimal band ratio (x-axis). Data collected on 17 August 2021 at the Gold Creek and Bear Gulch site represented by red circles and green squares, respectively, while data collected on 9 September 2021 are shown with blue diamonds.
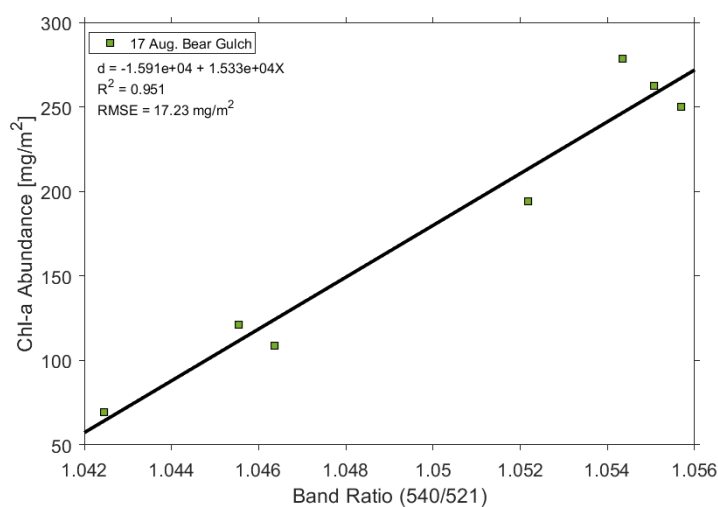
Figure S5. Analytics from the regression analysis of epilithic phycocyanin standing crops from the combined (all field sites) data set.

(a) Heat map of R^2 values generated by fitting each band combination against total chl *a* standing crops. Colors within the heat map represent the R^2 value, with wavelength numerators and denominators shown on the x- and y-axes, respectively.
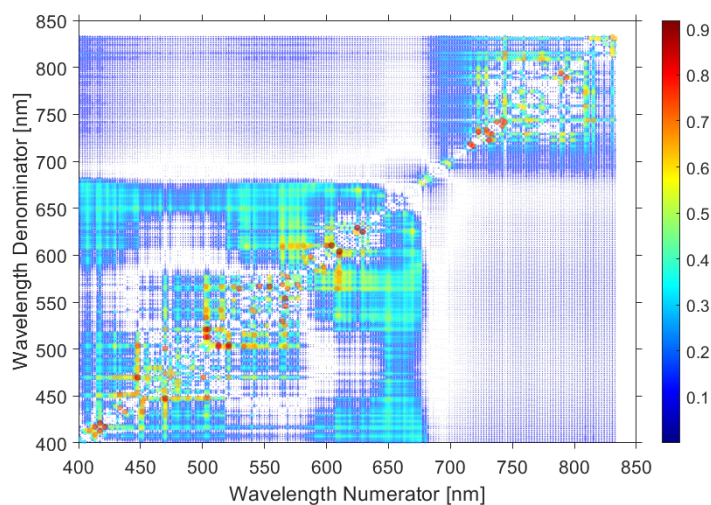

(b) Histogram of the R^2 values generated using the brute-force analysis.
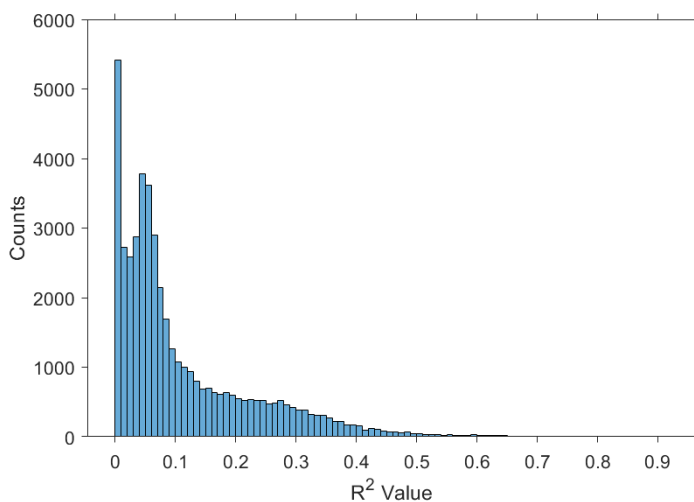

(c) Linear regression analysis between total chl *a* abundance (y-axis) and optimal band ratio (x-axis). Data collected on 17 August 2021 at the Bear Gulch site represented by green squares.

Figure S6. Analytics from the regression analysis of total chl *a* standing crops from the Bear Gulch data set.
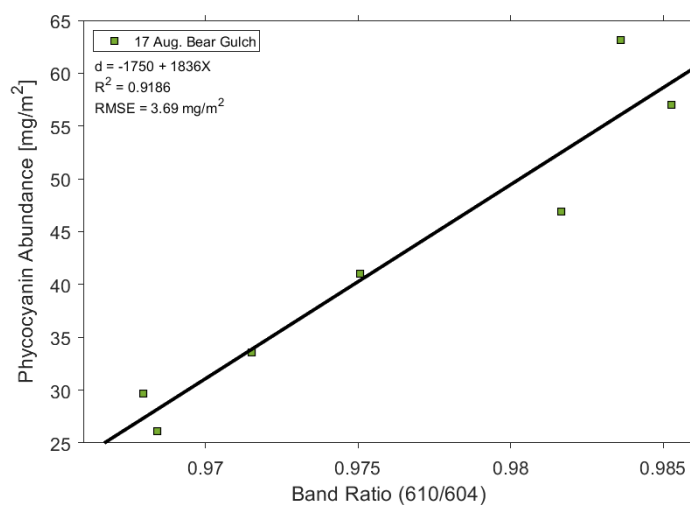
(a) Heat map of R^2 values generated by fitting each band combination against total phycocyanin standing crops. Colors within the heat map represent the R^2 value, with wavelength numerators and denominators shown on the x- and y-axes, respectively.
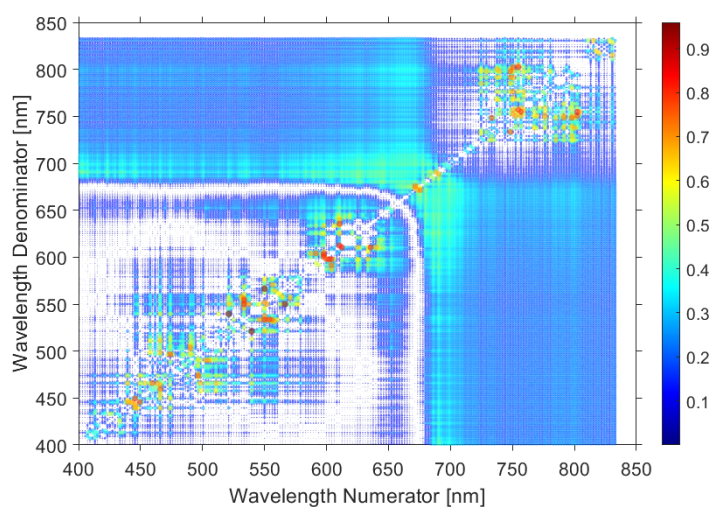

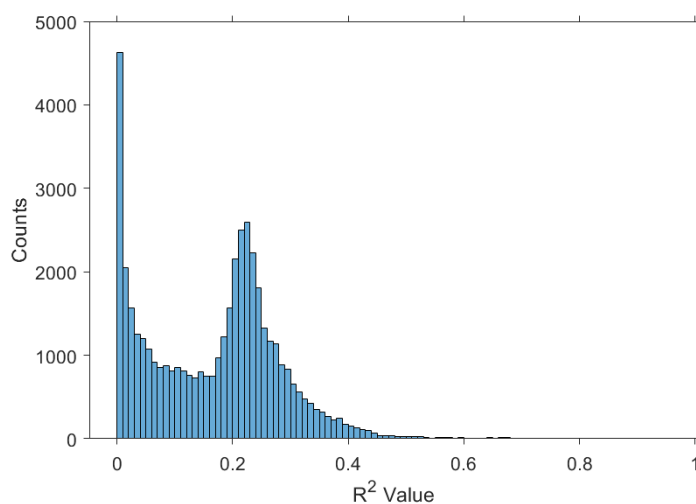(b) Histogram of the R^2 values generated using the brute-force analysis.

(c) Linear regression analysis between total phycocyanin abundance (y-axis) and optimal band ratio (x-axis). Data collected on 17 August 2021 at the Bear Gulch site represented by green squares.

Figure S7. Analytics from the regression analysis of total phycocyanin standing crops from the Bear Gulch data set.
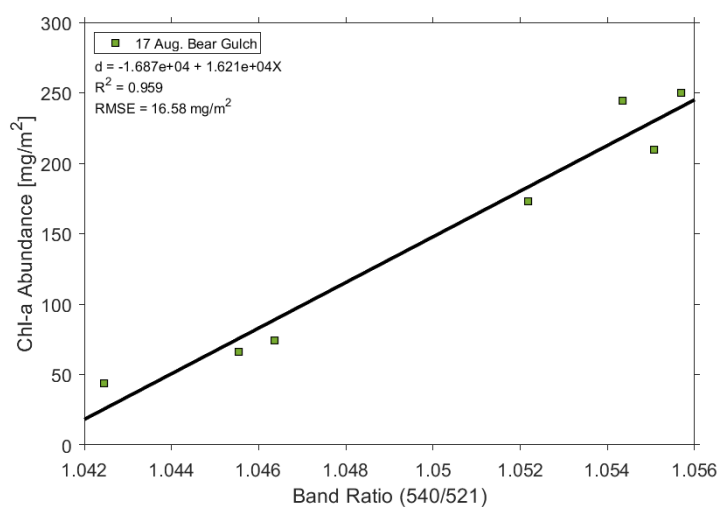
(a) Heat map of R^2 values generated by fitting each band combination against fila/epip chl *a* standing crops. Colors within the heat map represent the R^2 value, with wavelength numerators and denominators shown on the x- and y-axes, respectively.
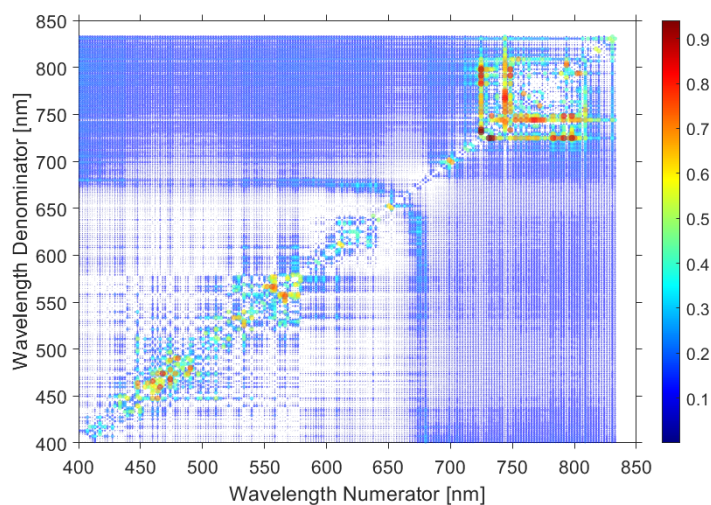
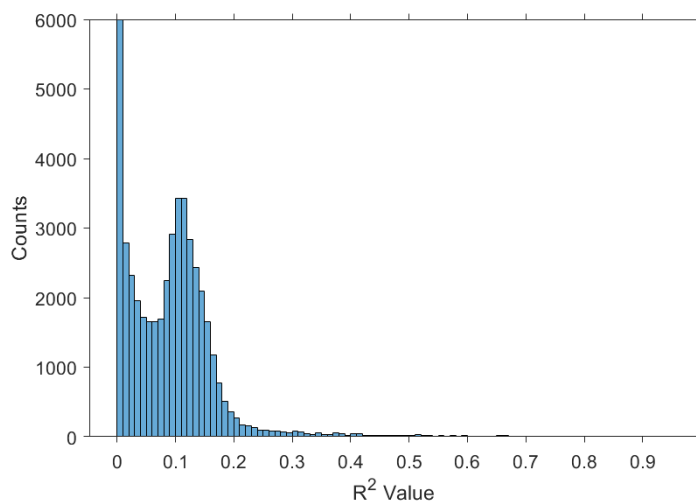(b) Histogram of the R^2 values generated using the brute-force analysis.

(c) Linear regression analysis between fila/epip chl *a* abundance (y-axis) and optimal band ratio (x-axis). Data collected on 17 August 2021 at the Bear Gulch site represented by green squares.
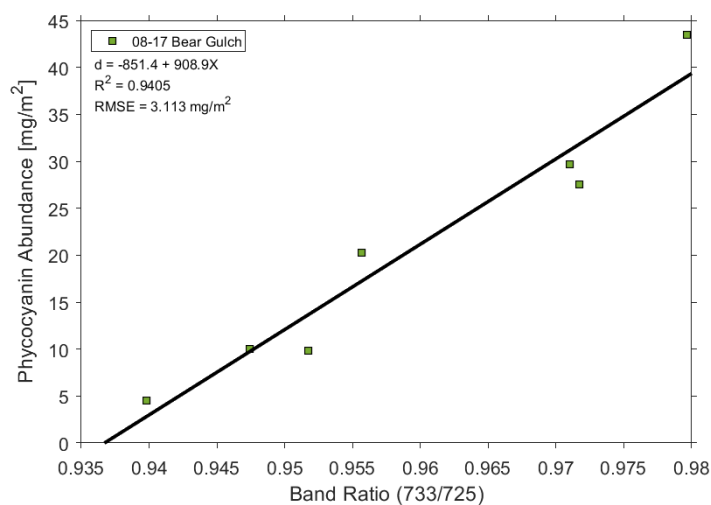
Figure S8. Analytics from the regression analysis of fila/epip chl *a* standing crops from the Bear Gulch data set.

(a) Heat map of R^2 values generated by fitting each band combination against epiphytic phycocyanin standing crops. Colors within the heat map represent the R^2 value, with wavelength numerators and denominators shown on the x- and y-axes, respectively.
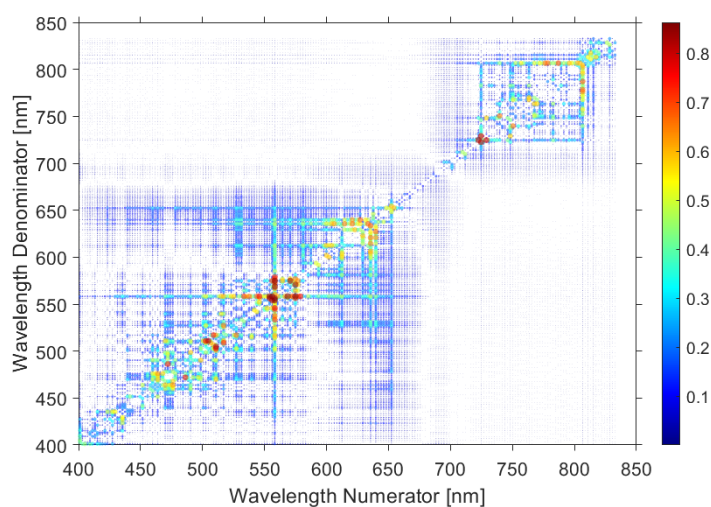

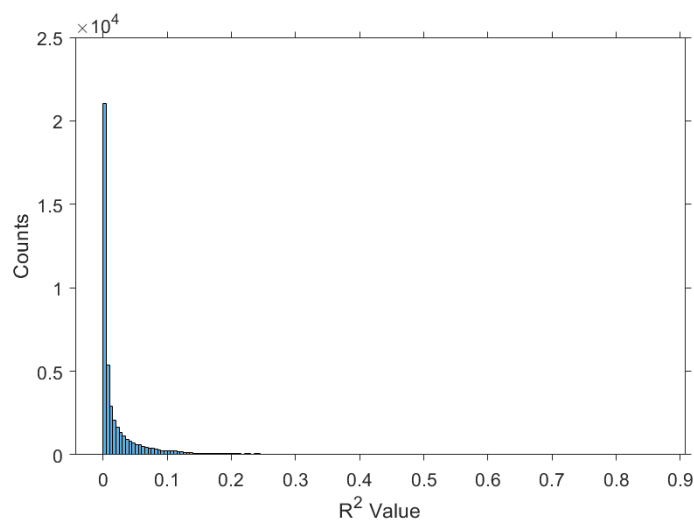(b) Histogram of the R^2 values generated using the brute-force analysis.

(c) Linear regression analysis between epiphytic phycocyanin abundance (y-axis) and optimal band ratio (x-axis). Data collected on 17 August 2021 at the Bear Gulch site represented by green squares.
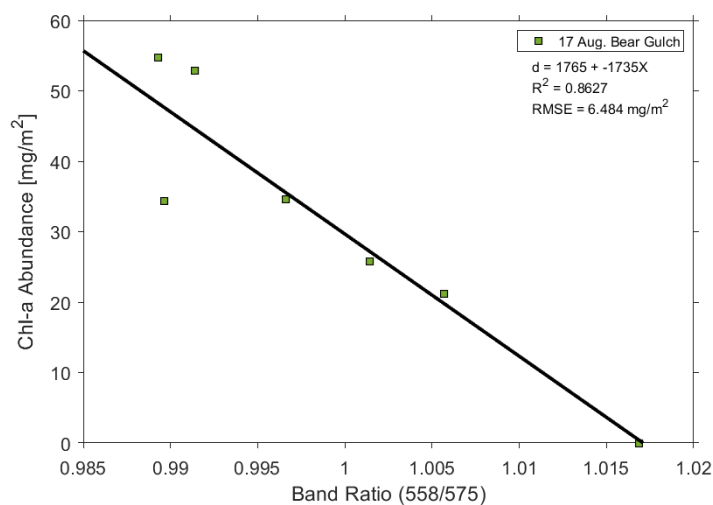
Figure S9. Analytics from the regression analysis of epiphytic phycocyanin standing crops from the Bear Gulch data set.

(a) Heat map of R^2 values generated by fitting each band combination against epilithic chl *a* standing crops. Colors within the heat map represent the R^2 value, with wavelength numerators and denominators shown on the x- and y-axes, respectively.
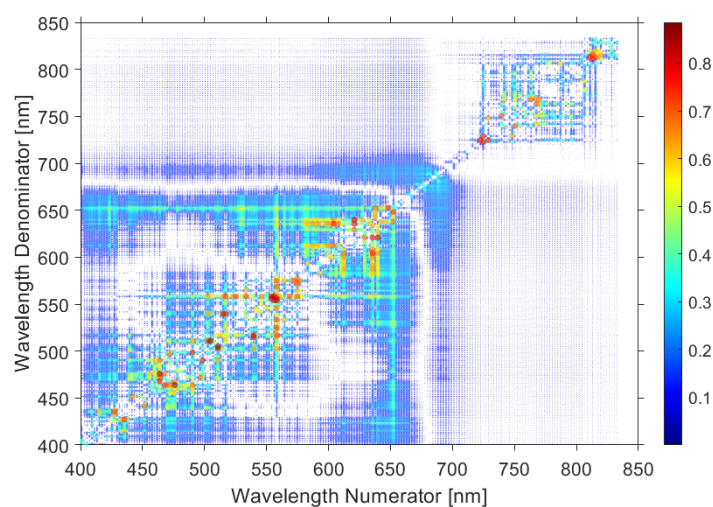

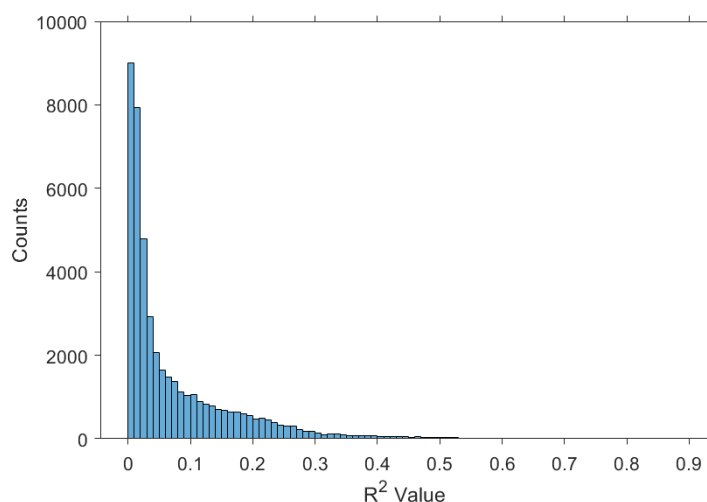(b) Histogram of the R^2 values generated using the brute-force analysis.

(c) Linear regression analysis between epilithic chl *a* abundance (y-axis) and optimal band ratio (x-axis). Data collected on 17 August 2021 at the Bear Gulch site represented by green squares.
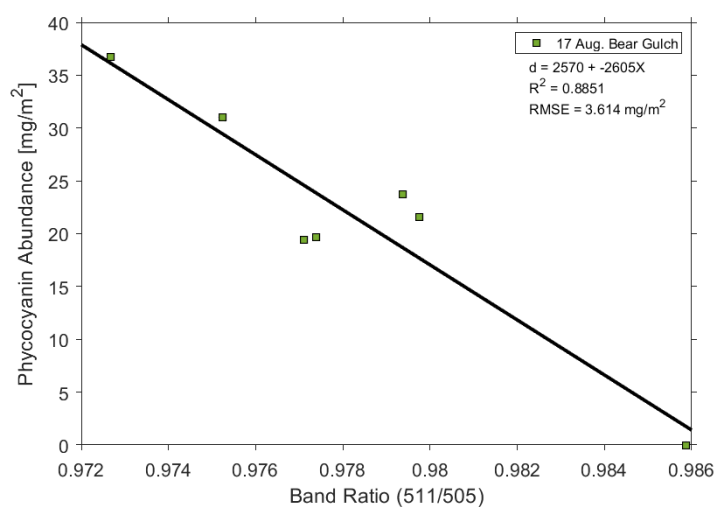
Figure S10. Analytics from the regression analysis of epilithic chl *a* standing crops from the Bear Gulch data set.

(a) Heat map of R^2 values generated by fitting each band combination against epilithic phycocyanin standing crops. Colors within the heat map represent the R^2 value, with wavelength numerators and denominators shown on the x- and y-axes, respectively.
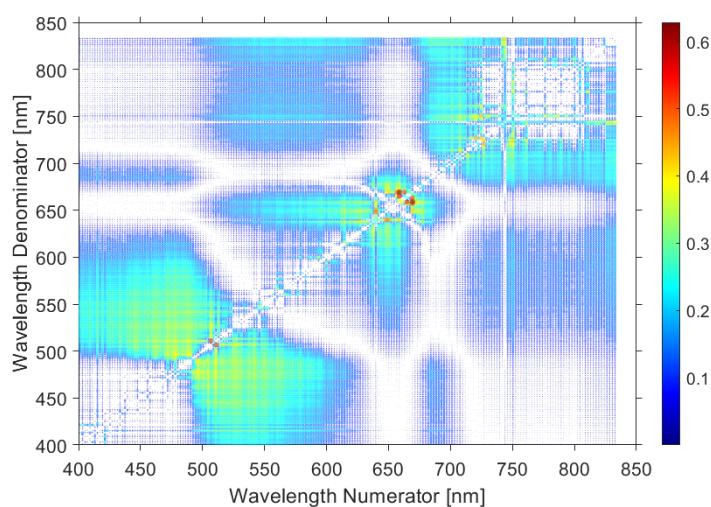

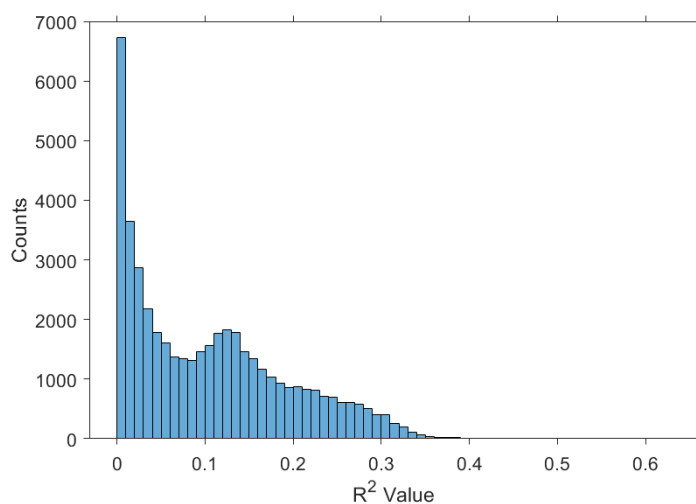(b) Histogram of the R^2 values generated using the brute-force analysis.

(c) Linear regression analysis between epilithic phycocyanin abundance (y-axis) and optimal band ratio (x-axis). Data collected on 17 August 2021 at the Bear Gulch site represented by green squares.
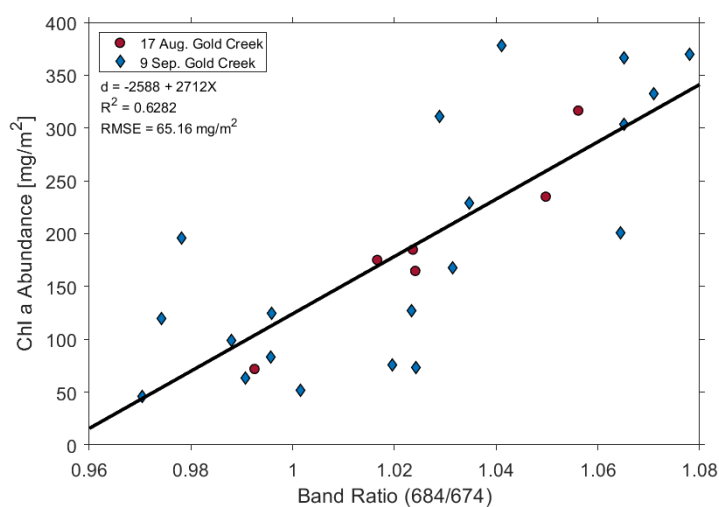
Figure S11. Analytics from the regression analysis of epilithic phycocyanin standing crops from the Bear Gulch data set.

(a) Heat map of R^2 values generated by fitting each band combination against total chl *a* standing crops. Colors within the heat map represent the R^2 value, with wavelength numerators and denominators shown on the x- and y-axes, respectively.
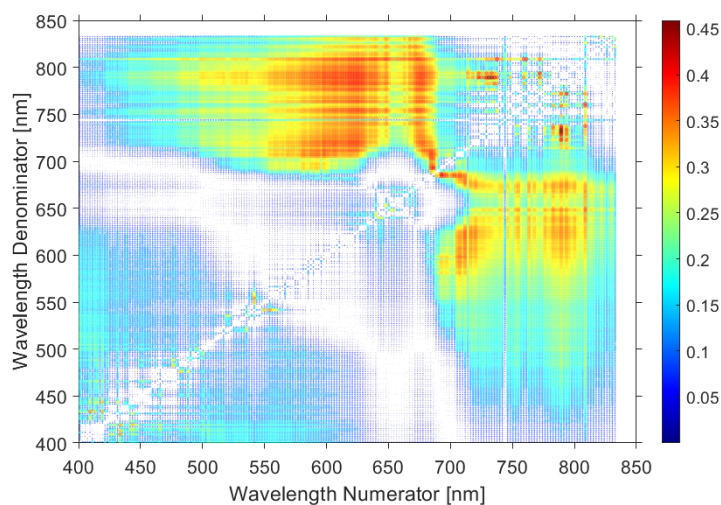

(b) Histogram of the R^2 values generated using the brute-force analysis.
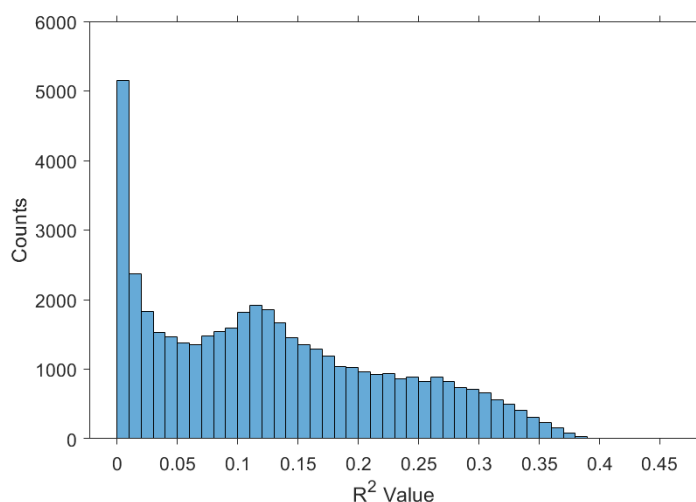

(c) Linear regression analysis between total chl *a* abundance (y-axis) and optimal band ratio (x-axis). Data collected on 17 August 2021 at the Gold Creek site represented by red circles, while data collected on 9 September 2021 are shown with blue diamonds.
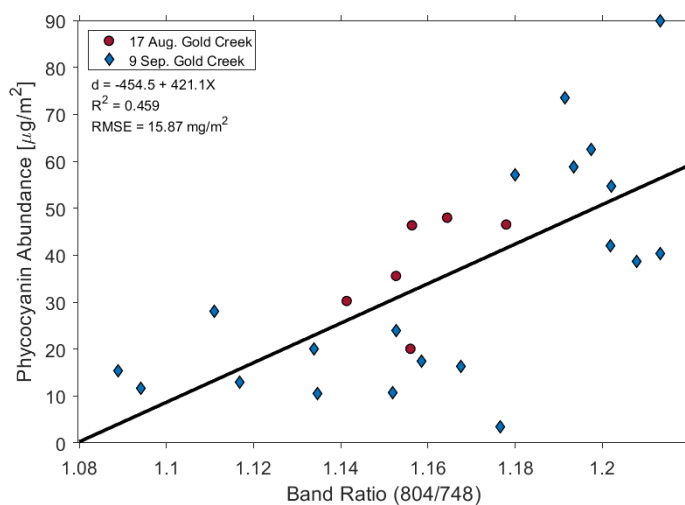
Figure S12. Analytics from the regression analysis of total chl *a* standing crops from the Gold Creek data set.

(a) Heat map of R^2 values generated by fitting each band combination against total phycocyanin standing crops. Colors within the heat map represent the R^2 value, with wavelength numerators and denominators shown on the x- and y-axes, respectively.
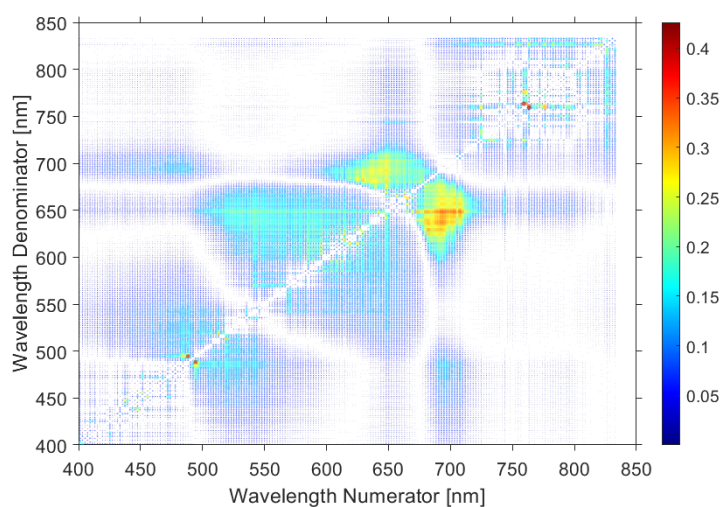

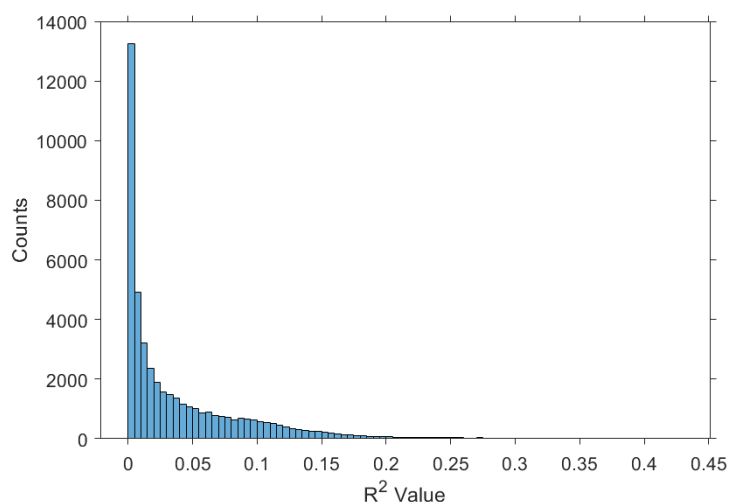(b) Histogram of the R^2 values generated using the brute-force analysis.

(c) Linear regression analysis between total phycocyanin abundance (y-axis) and optimal band ratio (x-axis). Data collected on 17 August 2021 at the Gold Creek site represented by red circles, while data collected on 9 September 2021 are shown with blue diamonds.

Figure S13. Analytics from the regression analysis of total phycocyanin standing crops from the Gold Creek data set.
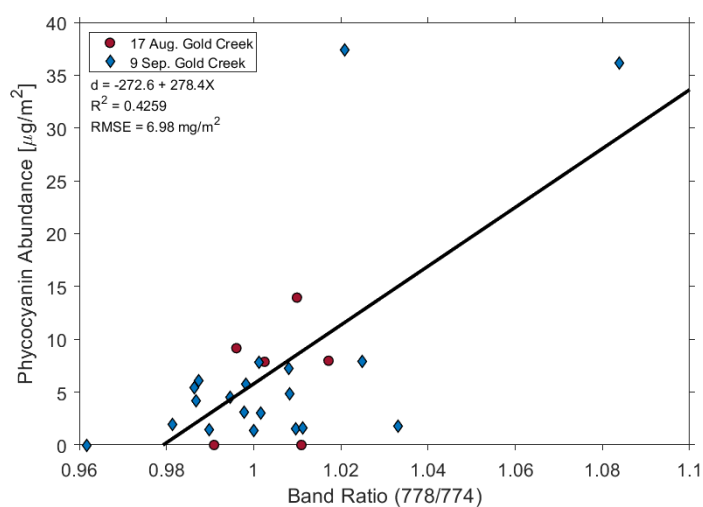
(a) Heat map of R^2 values generated by fitting each band combination against epiphytic phycocyanin standing crops. Colors within the heat map represent the R^2 value, with wavelength numerators and denominators shown on the x- and y-axes, respectively.
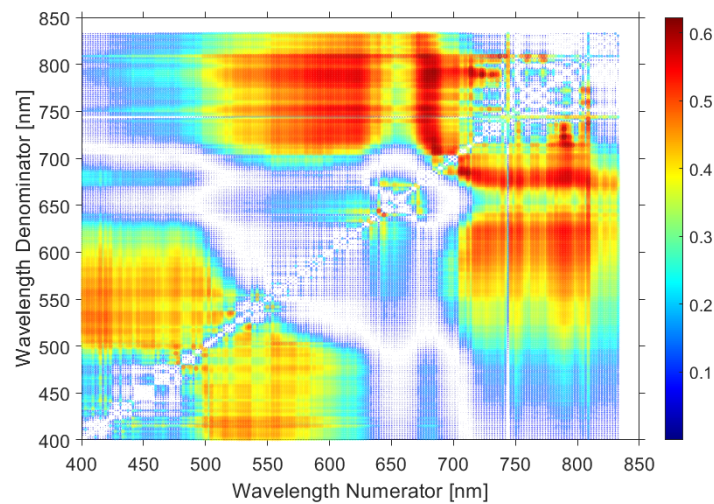

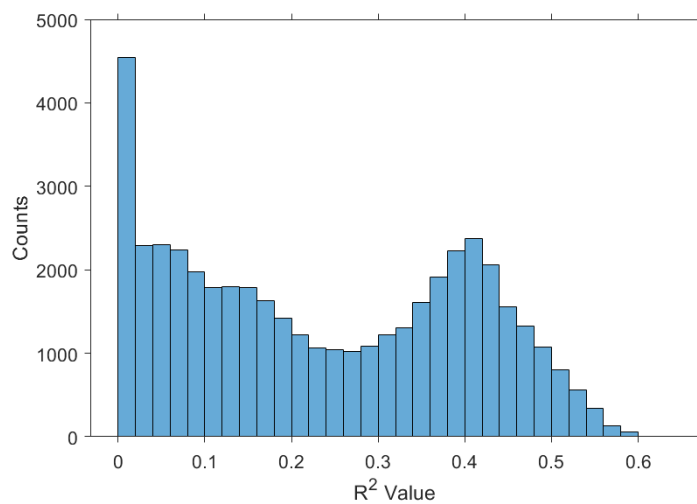(b) Histogram of the R^2 values generated using the brute-force analysis.

(c) Linear regression analysis between epiphytic phycocyanin abundance (y-axis) and optimal band ratio (x-axis). Data collected on 17 August 2021 at the Gold Creek site represented by red circles, while data collected on 9 September 2021 are shown with blue diamonds.

Figure S14. Analytics from the regression analysis of epiphytic phycocyanin standing crops from the Gold Creek data set.
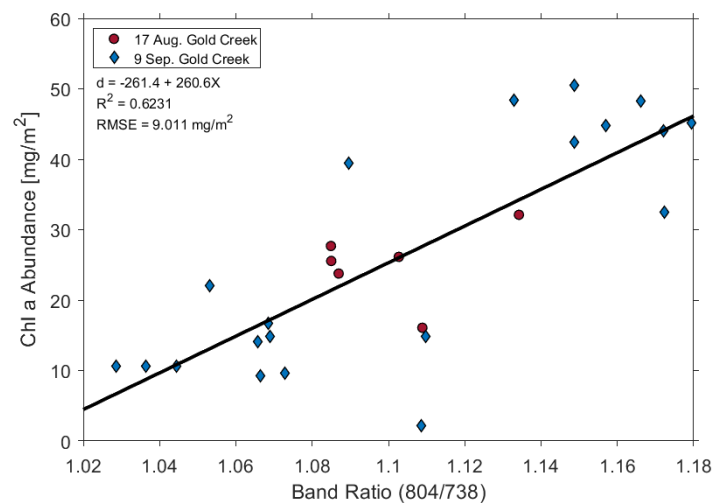
(a) Heat map of R^2 values generated by fitting each band combination against epilithic chl *a* standing crops. Colors within the heat map represent the R^2 value, with wavelength numerators and denominators shown on the x- and y-axes, respectively.

(b) Histogram of the R^2 values generated using the brute-force analysis.

(c) Linear regression analysis between epilithic chl *a* abundance (y-axis) and optimal band ratio (x-axis). Data collected on 17 August 2021 at the Gold Creek site represented by red circles, while data collected on 9 September 2021 are shown with blue diamonds.

Figure S15. Analytics from the regression analysis of epilithic chl *a* standing crops from the Gold Creek data set.